1.Classification *INPE-COM.10/PE*	2.Period	4.Distribution Criterion internal ☐ external X
3.Key Words (selected by the author) *IMAGE PROCESSING* *EDGE DETECTION* *STATISTICAL DECISION THEORY*		
5.Report No. *INPE-1194-PE/111*	6.Date *February, 1978*	7.Revised by José Sobral *J. H. A. Sobral*
8. Title and Sub-title *EDGE DETECTION IN IMAGES: A HYPOTHESIS TESTING APPROACH*		9.Authorized by Parada *Nelson de Jesus Parada* *Director*
10.Sector Code		11.No. of Copies *10*
12.Authorship *Nelson D. A. Mascarenhas* *Lucila O.C. Prado* Nelson Dellino d'Avila Mascarenhas 13.Signature of first author		14.No. of Pages *25* 15.Price

16.Summary/Notes

New statistical techniques for the edge detection problem in images are developed. The image is modeled by signal and noise which are independent, additive, Gaussian and autorregressive in two dimensions. The optimal solution, in terms of statistical decision theory, leads to a test which decides among multiple, composite, overlapping hypotheses. A computationally attractive suboptimal test, involving non-overlapping hypotheses, is proposed. Results are presented with simulated data and real satellite images. A comparison with standard gradient techniques is made.

17.Remarks *To be presented at the 14th International Conference on Pattern Recognition, Kyoto, Japan.*

INDEX

1 - INTRODUCTION

The problem of edge detection has been of considerable interest in visual pattern recognition. However, the proposed methods are often heuristic. Techniques involving differentiation, like the gradient or the laplacian are highly susceptible to noise. A few statistical methods for detecting edges have been proposed. Nahi and Habibi [1] used a replacement process to decide if a picture element belongs to the object or to the background. Modestino and Fries [2] used two dimensional recursive digital filtering structures.

The method that is proposed in this article is based on statistical decision theory and it takes explicitly into consideration the randomness of signal and noise in a formal way. Moreover, the algorithm can be implemented with computational effort that is at least comparable to those techniques involving derivatives.

2 - STATEMENT OF THE PROBLEM

The statistical algorithm adopts the following two dimensional autoregressive model for the signal [3]:

$$s(k+1, \ell+1) = \rho_1 s(k+1, \ell) + \rho_2 s(k, \ell+1) - \rho_1 \rho_2 s(k, \ell) + \sqrt{(1-\rho_1^2)(1-\rho_2^2)}\; U(k, \ell) \qquad (1)$$

In this model the random variables have null means; ρ_1 (ρ_2) is the correlation coefficient between non-noisy pixels on the horizontal (vertical) directions; $\{U(k,\ell)\}$ is a set of non-correlated random variables, with the same variance as $\{s(k+1, \ell+1)\}$.

We adopt the hypothesis of Gaussian signal. Although this is not completely true, such adoption allows us to establish a

mathematically tractable model which has the additional feature of being easy to be determined experimentally, since it only requires estimation of means and covariances between pixels.

The noise in the image comes from several sources, as stated earlier. In order to keep the model tractable, it is convenient to assume that this noise is Gaussian, additive, independent of the signal and also described by Eq. (1).

Once the models for signal and noise are set, the next step is to adequately define the edge detection problem. This definition should be simple and yet it should take into consideration what an edge means in psychophysical terms.

Under this perspective, the edge detection problem is proposed in the following terms: having observed four noisy pixels $v(i, j)$, $v(i, j+1)$, $v(i+1, j)$ and $v(i+1, j+1)$, like in Fig. 1, where $v(k, \ell) = s(k, \ell) + n(k, \ell)$, that is, noisy signal = signal + noise, we want to take a decision with respect to the signal without noise.

This formulation of the problem in terms of statistical decision theory leads to a set of seven possible hypotheses:

$$1) \left| s(i, j) - \frac{s(i, j+1) + s(i+1, j) + s(i+1, j+1)}{3} \right| \gtrless \Delta$$

$$2) \left| s(i, j+1) - \frac{s(i, j) + s(i+1, j) + s(i+1, j+1)}{3} \right| \gtrless \Delta$$

$$3) \left| s(i+1, j) - \frac{s(i, j) + s(i, j+1) + s(i+1, j+1)}{3} \right| \gtrless \Delta$$

$$4) \left| s(i+1, j+1) - \frac{s(i, j) + (i, j+1) + s(i+1, j)}{3} \right| \gtrless \Delta$$

$$5)\ \left| \frac{s(i,j)+s(i,j+1)}{2} - \frac{s(i+1,j)+s(i+1,j+1)}{2} \right| \geq \Delta$$

$$6)\ \left| \frac{s(i,j)+s(i+1,j)}{2} - \frac{s(i,j+1)+s(i+1,j+1)}{2} \right| \geq \Delta$$

$$7)\ \left| s(i,j) - \frac{s(i,j+1)+s(1+1,j)+s(i+1,j+1)}{3} \right| < \Delta$$

$$\cap \left| s(i,j+1) - \frac{s(i,j)+s(i+1,j)+s(i+1,\ j+1)}{3} \right| < \Delta$$

$$\cap \left| s(i+1,j) - \frac{s(i,j)+s(i,j+1)+s(i+1,j+1)}{3} \right| < \Delta$$

$$\cap \left| s(i+1,j+1) - \frac{s(i,j)+s(i,j+1)+s(i+1,j)}{3} \right| < \Delta$$

$$\cap \left| \frac{s(i,j)+s(i,j+1)}{2} - \frac{s(i+1,j)+s(i+1,j+1)}{2} \right| < \Delta$$

$$\cap \left| \frac{s(i,j)+s(i+1,j)}{2} - \frac{s(i,j+1)+s(i+1,j+1)}{2} \right| < \Delta \quad (2)$$

The non-negative parameter Δ allows one to adjust the result of the decision to a visual judgement, with some interaction with the machine, through a computer display.

Hypotheses 1 to 6 correspond, respectively, to existence of edges according to diagonal (Figs. 2 to 5), horizontal (Fig. 6) and vertical (Fig. 7) directions and hypothesis 7 corresponds to non--existence of edge.

Proposed as such, the edge detection problem is reduced to the solution of a multiple hypotheses problem. Moreover, these hypotheses are composite (since each of them involves a region in the space of the signal) and they overlap since, for example, the set of

non-noisy pixels (Fig. 8) satisfies hypotheses 1, 2 and 5, for $\Delta = 0.5$. In the next two sections, solution methods for this hypothesis testing problem will be developed.

3 - OPTIMAL SOLUTION

The statistical decision problem presented in the previous section will be solved by adopting the Bayesian point of view. Fig. 9 illustrates the diagram of the model. We want to partition the observation space V, that is, to choose the optimal decision rule.

$\sigma(s)$ defines the probability density function of the non-noisy signal; $f(v/s)$ gives the probability density function of the noisy signal, conditioned upon the value of the non-noisy signal; with respect to $d(\gamma/v)$, it is well known that nothing is gained by admitting a randomized decision rule. Therefore, the space V will be partitioned in seven regions, corresponding to the seven possible decisions. It is easy to show that, by selecting appropriate cost functions $C(s, \gamma_i)$, $i=1, 2, \text{---}, 7$, the overall risk is minimized by selecting the decision γ_i that correspondes to the minimal value of

$$A_i(v) = \int_S C(s, \gamma_i)\, f(v/s)\, \sigma(s)\, ds \qquad (3)$$

Although the problem is close to the theoretical solution, there is a significant point to be considered: the fact that the hypotheses overlap. One can imagine the space S as being partitioned into two regions: a) hypothesis 7 (non-edge), which is disjoint of the other six hypotheses by definition; b) hypotheses 1 to 6 which overlap each other.

Ogg [4] and Middleton [5] proposed the following cost function to solve the overlapping hypotheses testing problem:

$$C(s, \gamma_i) = \frac{\sum_{j=1}^{7} c(\gamma_i, j)\, P_j\, W_j(s)}{\sum_{j=1}^{7} P_j\, W_j(s)} \tag{4}$$

where $P_j = \int_{\text{region } j} \sigma(s)\, ds$ is the a priori probability associated with hypothesis j, $W_j(s)$ is the conditional probability density function of s, given hypothesis j and $c(\gamma_i, j)$ is the cost to decide for hypothesis γ_i, when we consider class j.

Using these cost functions, one obtains:

$$A_i(v) = \sum_{j=1}^{7} c(\gamma_i, j) \int_{\text{region } j} \sigma(s)\, f(v/s)\, ds \tag{5}$$

If the following costs $c(\gamma_i, j)$ are selected:

$$c(\gamma_i, j) = \begin{cases} 1, & \text{if } i \neq j \\ 0, & \text{if } i = j \end{cases} \tag{6}$$

it follows that:

$$A_i(v) = \sum_{\substack{j=1 \\ j \neq i}}^{7} \int_{\text{region } j} \sigma(s)\, f(v/s)\, ds \tag{7}$$

We must take the minimum value for $A_i(v)$, $i = 1, 2, \ldots, 7$. It is easy to see that $A_i(v)$ will be minimum if

$\int_{\text{region } i} \sigma(s)\, f(v/s)\, ds$ is maximum. The final decision, for the costs

given by (6), would consist in performing seven integrals of the last type and to consider the largest of them.

Although the edge detection problem is now formally solved, there are still computational obstacles that have to be removed. First, integrations in a four dimensional space must be made. The integration over the region that defines the seventh hypothesis (non-existence of edge) is difficult to be numerically computed, since this region is not regular, being defined by the intersection of regular regions. The next section will show the development of a suboptimal solution to the problem, that will circumvent this difficulty.

4 - SUBOPTIMAL SOLUTION

The computational problems involved in the optimal solution led us to develop the following scheme: one would first take binary decisions involving non-overlapping hypotheses of the type edge versus non-edge of the same type. Then the results of the preliminary tests would be compared and the final decision would be taken. This scheme can be illustrated by Fig. 10.

This type of formulation tends to favor the acceptance of non-edge hypothesis, for two reasons:

a) the integration $\int_{\text{region non-edge}} \sigma(s)\, f(v/s)\, ds$ in each binary decision is made over a region that is larger than the one that is used in the optimal solution because in the latter scheme the region that defines the hypothesis non-edge is an intersection of areas. Observe that the regions that define the non-edge hypothesis are different in each of the preliminary tests;

b) the non-edge hypothesis appears in all six preliminary tests, while any other hypothesis shows up in only one of them.

This preferential treatment of the non-edge hypothesis can be somehow compensated by increasing the cost of choosing it when the edge hypothesis is true in the partial tests.

The derivation of the decision procedure for each binary detection problem can start with Eq. (3) which is general, not depending upon the fact that the hypotheses overlap or not. In this situation, there are two hypotheses, edge of a certain type versus non-edge of the same type and we have two functions A_1 (v) and A_2 (v).

Since the hypotheses do not overlap, one can take as cost functions C (s, γ_i) constant values c_{ij}, where the first and second indexes denote the true and the chosen hypotheses, respectively. Index 0 (zero) represent hypothesis non-edge of a certain type and index 1 (one) denotes edge of the same type. Therefore, the final decision is given by:

$$\frac{\int_{||\geq\Delta} \sigma\,(s)\, f\,(v/s)\, ds}{\int_{||<\Delta} \sigma\,(s)\, f\,(v/s)\, ds} \underset{0}{\overset{1}{\gtrless}} \frac{C_{01} - C_{00}}{C_{10} - C_{11}} \tag{8}$$

where 1 denotes decision for an edge of a certain type and 0 denotes decision for non-edge.

Therefore, the classical Bayesian test, that decides between two composite hypotheses involving a likelihood ratio, is obtained [6].

Once the binary decisions are taken, involving edge versus non-edge of a certain type, the final decision about which type of edge (or non-edge) is chosen (Fig. 10) has to be made. For this, we will associate with the accepted hypotheses in the preliminary test the value:

$$\frac{C_{10} - C_{11}}{C_{01} - C_{00}} \qquad \frac{\int_{||} \sigma(s)\, f(f/s)\, ds}{\int_{||} \sigma(s)\, f(v/s)\, ds} \qquad \begin{matrix} ||\geq \Delta \\ ||> \Delta \end{matrix} \tag{9}$$

or its inverse, whether this value would be greater or equal (there is an edge) or less (there is non-edge) than one. We will accept the hypothesis associated with the highest value. Observe that the non-edge hypothesis can furnish up to six candidates for the final decision.

The modeling of signal and noise as Gaussian processes allows the specification of the densities $\sigma(s)$ and $f(v/s)$ through their mean vectors (assumed zero by subtracting the sample mean of the image before processing) and covariance matrix.

The computational implementation of the likelihood ratio test may demand the construction and the follow-up of tables which avoid the necessity of repeating the numerical calculation of the integrals.

From the symmetry of the problem. it is only necessary to compute two tables, corresponding to hypotheses 1 and 5 (edges at 45^{o} and horizontal). However, these tests depend on tables with four entry variables and this computational effort may turn the algorithm unfeasible. In the next section, a development of a computationally attractive approximation to the suboptimal solution of the problem is introduced.

5 - APPROXIMATION TO THE SUBOPTIMAL SOLUTION

In order to make feasible the solution of the edge detection problem, it is necessary to make a second approximation. This will be done by renouncing to the examination of the four noisy pixels in order to take the decision. Only two random variables will be observed.

Therefore, to decide edge of type 1 against non-edge of type 1 (edge at 45^{o}) the algorithm, instead of observing v (i,j), v (i, j + 1), v (i + 1, j) and v (i + 1, j + 1), will observe only v (i, j) and $\frac{v\,(i,\,j+1) + v\,(i+1,\,j) + v\,(i+1,\,j+1)}{3}$. Likewise, in the test edge type 5 (horizontal edge) versus non-edge of the same type, the likelihood functions will depend on $v\,\frac{(i,\,j) + v\,(i,\,j+1)}{2}$ and $\frac{v\,(i+1,\,j) + v\,(i+i,\,j+1)}{2}$. As a result, the necessary tables will depend only on two variables, which clearly reduces considerably the computational task. Therefore, in the case of edge of type 1, the denominator of expression (8) assumes the form:

$$\int_{|\,|\,<\,\Delta} \sigma\,(s(i,j),\ s(i,j+1),\ s(i+1,j),\ s(i+1,\ j+1))\ f\ (\ (v(i,j),\ \frac{v(i,j+1) + v(i+1,j) + v(i+1,\ j+1)}{3})\ |s(i,j),\ s(i,j+1),\ s(i+1,j),$$

$$s(i+1,\ j+1))\ ds(i,j)\ ds(i,j+1)\ ds(i+1,j)\ ds(i+1,\ j+1) \qquad (10)$$

6 - SIMPLIFICATION OF THE INTEGRAL COMPUTATION

Let us use the following notation: $s_1 = s(i,j)$, $s_2 = s(i,j+1)$, $s_3 = s(i+1,j)$, $s_4 = s(i+1,\ j+1)$, $s' = (s_2 + s_3 + s_4) : 3$, $v_1 = v(i,j)$, $v' = (v(i,j+1) + v(i+1,j) + v(i+1,\ j+1)) : 3$. Under these conditions, expression (10) assumes the form:

$$\int\int\int\int f(v_1, v'\,|s_1\ s_2\ s_3\ s_4)\ f_{S_1\ S_2\ S_3\ S_4}\ (s_1,\ s_2,\ s_3,\ s_4)\cdot \cdot ds_1\ ds_2\ ds_3\ ds_4$$

$$|s_1 - \frac{s_2 + s_3 + s_4}{3}| < \Delta \qquad (11)$$

It can be shown [7] that in the Gaussian case, expression (11) can be obtained by performing only a double integration, instead of a quadruple integration, that is, Eq. (11) can be given by:

$$\int_{-\infty}^{\infty} ds_1 \int_{s_1 - \Delta}^{s_1 + \Delta} ds' \; f(v_1, v' \mid s_1 s') \; f_{S_1 S'}(s_1, s') \qquad (12)$$

This result reduces considerably the computational effort of numerical integration.

7 - NUMERICAL COMPUTATION OF THE INTEGRALS

Eq. (8) specifies the likelihood ratio test, which demands the computation of integrals in the numerator and the denominator. The denominator given by:

$$\int_{||<\Delta} \sigma(s) \, f(v/s) \, ds \quad \text{can be calculated by}$$

$$\int_{-\infty}^{\infty} ds_\alpha \int_{s_\alpha - \Delta}^{s_\alpha + \Delta} ds_\beta \; \sigma(s_\alpha, s_\beta) \, f(v_\alpha, v_\beta \mid s_\alpha, s_\beta) \qquad (13)$$

where

$$v_\alpha = v(i, j),$$
$$s_\alpha = s(i, j),$$
$$v_\beta = (v(i,j+1) + v(i+1,j) + v(i+1, j+1)):3,$$
$$s_\beta = (s(i,j+1) + s(i+1,j) + s(i+1,j+1)):3$$

in the case of the test of type 1 (diagonal edge), for example. An analogous expression is used with tests type 2, 3 and 4. For test type 5 (horizontal edge), we have:

$$v_\alpha = (v(i,j) + v(i,j+1)) : 2,$$

$$s_\alpha = (s(i,j) + s(i,j+1)) : 2,$$

$$v_\beta = (v(i+1,j) + v(i+1, j+1)) : 2,$$

$$s_\beta = (s(i+1,j) + s(i+1, j+1)) : 2.$$

An analogous convention can be used with test type 6 (vertical edge).

The numerator of Eq. (8), given by $\int_{|\,| \geq \Delta} \sigma\,(s)\, f\,(v/s)$, can be calculated by:

$$\int_{-\infty}^{\infty} ds_\alpha \int_{-\infty}^{s_\alpha - \Delta} ds_\beta\, \sigma\,(s_\alpha, s_\beta)\, f\,(v_\alpha, v_\beta | s_\alpha, s_\beta) +$$

$$\int_{-\infty}^{\infty} ds_\alpha \int_{s_\alpha + \Delta}^{\infty} ds_\beta\, \sigma\,(s_\alpha, s_\beta)\, f\,(v_\alpha, v_\beta \mid s_\alpha, s_\beta) \qquad (14)$$

Under de hypothesis of signal and noise being Gaussian, those integrals have the general form [8]:

$$K \cdot \int_{-\infty}^{\infty} dx \exp(-x^2) \frac{1}{\sqrt{2\pi}} \int_a^b \exp(-y^2/2)\, dy \qquad (15)$$

In the case of Eq. (13), $\underline{a}$ and $\underline{b}$ are finite; in the first term of Eq. (14), $\underline{a} = -\infty$ and b is finite, while in the second term, $\underline{a}$ is finite and $\underline{b} = +\infty$. The integration

$$\frac{1}{\sqrt{2\pi}} \int_a^b dy \exp(-y^2/2)$$

is performed by storing a Gaussian distribution table. The integration from $-\infty$ to $+\infty$ then can be put in the form:

$$K \cdot \int_{-\infty}^{\infty} dx \ \exp(-x^2)\ f(x) \tag{16}$$

This integral can be numerically calculated through the application of the Gauss-Hermite formula [9].

$$\int_{-\infty}^{\infty} dx \exp(-x^2)\ f(x) \simeq \sum_{K=1}^{m} H_K\ f(x_K) \tag{17}$$

where x_K is the K-th zero of the Hermite polynomial $H_m(x)$, of the $m^{\underline{th}}$ degree, and the weights H_K are given by:

$$H_K = \frac{2^m\ (m-1)!\ \sqrt{\pi}}{H'_m(x_K)\ H_{m-1}(x_K)} \tag{18}$$

Values of x_K and H_K are given by table [10]

8 - EXPERIMENTAL RESULTS

To test the proposed algorithm, a simulation work was performed on a cartoon image of size 128 x 128 with 9 gray levels (Fig. 11). White Gaussian noise was added to the image, under different signal to noise ratios; 20 roots were used when performing the Gauss--Hermite integration and a normal distribution with precision up to 6.8 standard deviations was stored.

Initially, the scanning was performed by examining non--overlapping blocks of four pixels. As a result, some edges were not detected since they were located exactly in between the blocks. In order to eliminate this problem, a modification was made on the type of scanning, superimposing adjacent groups of observed pixels and reducing the number of hypotheses from 7 to 5, in order to avoid an excessive

amount of computation, according to Figs. 12, 13, 14 and 15. Hypothesis 5 corresponds to non-existence of edge.

With this new scheme, the problem of missing intermediate edges is avoided at the price of an increased computational effort, since, with the original type of scanning, the number of tests to be performed is proportional to $\frac{M^2}{4} \cdot 6$ (where M^2 is the number of pixels of the image) while in the second type of scanning this number is proportional to $M^2 \cdot 4$. Furthermore, the tests of diagonal edges involving individual pixels (instead of averages) tend to have a greater probability of error. Nevertheless, the results under SNR (that is, the ratio of signal variance to noise variance) 100 (Figs. 16 and 17), 30 (Figs. 18 and 19), 10 (Figs. 20 and 21) and using the correlation coefficient of the signal equal to 0.96 (estimated from the original image), show that the algorithm is able to cope with noise quite effectively.

Decreasing the SNR further (SNR = 5) (Figs. 22 and 23) there is a tendency for the edges to disappear. This can be interpreted in terms of the fact that, for those values of the parameters, $P(D_o|H_1)$ is much higher than $P(D_1|H_o)$ in the binary tests, besides the preference given to the non-edge hypothesis, by being present in all these partial tests. This problem was solved by increasing the value of the cost C_{10} from 1.0 to 1.5 (see Fig. 24).

The superiority of the results of the proposed algorithm over the classical gradient procedure under noisy conditions can be observed through Fig. 25 (SNR = 10) and Fig. 26 (SNR = 5).

The CPU time for the 128 x 128 image using the overlapping scanning method with 5 hypotheses, on a B-6700 machine and Algol language, was 380 seconds when performing the likelihood ratios repeatedly by calculation, but this time was reduced to 24 seconds by the use of look-up tables.

The corresponding gradient procedure took 19 seconds. However, in the proposed method the edges are indicated by a gray level that depends on the ratio of the two greatest likelihood ratios of the partial tests. If we simply associate a dark tone to the existence of an edge and a light tone to the non-existence, it is possible to store in the look-up table only the information on which edge is decided and that requires only one entry (instead of four) in a table that uses a maximum of three bits of storage per pair of values, with considerable reduction in the computational task.

The proposed algorithm, under five hypotheses with overlap, was applied to detect edges on a 512 x 512 NOAA.V metereological satellite picture (Fig. 27), with 32 (Fig. 28) and 8 (Fig. 29) levels of quantization using as parameters $\rho_S = 0.90$, $\rho_N = 0$, SNR = 60 (the difference due to a greater quantization noise with 8 levels was not considered), $C_{10} = 10$, $\Delta = 0.90$ (32 levels) and $\Delta = 0.35$ (8 levels). These results show that, by attempting to preserve the number of quantization levels, some continuity of the edges seems to be lost. The construction of the table took approximately 2 minutes for 32 levels and a few seconds for 8 levels, while the execution time on a PDP 11/45 in Fortran demanded 20 minutes. The limited precision of the Gaussian table and of the floating point representation of the minicomputer forced some approximations.

This work will continue in the future, in the direction of incorporating contextual considerations, which may include the multispectral character of the images.

9 - CONCLUSIONS

A new algorithm to detect edges in images was developed, under the framework of statistical decision theory. This scheme takes explicitly into consideration the randomness of signal and noise. Suboptimal solutions were developed, with computational effort at least comparable to the classical procedures, like the gradient, and better performance under noisy conditions.

ACKNOWLEDGEMENTS

The authors wish to thank Dr. José Humberto de Andrade Sobral for his useful comments about the paper, and Mr. José Carlos Moreira for his help in the programming of the algorithm.

REFERENCES

[1] Nahi, N.E. and Habibi, A., Decision-Directed Recursive Image Enhancement, IEEE Transactions on Circuits and Systems, Vol. CAS-22, No. 3, March 1975, pp 286-293.

[2] Modestino, J.W. and Fries, R.W., Edge Detection in Noisy Images Using Recursive Digital Filtering, Joint Workshop on Pattern Recognition and Artificial Intelligence, 1976, pp 84-89.

[3] Habibi, A., Two Dimensional Bayesian Estimate of Images, Proceedings of the IEEE, Vol. 60, No. 7, 1972, pp 878-883.

[4] Ogg, Jr, F.C., A Note on Bayes Detection of Signals, IEEE Transactions on Information Theory, Vol. 10, No. 1, 1964, pp 57-60

[5] Middleton, D., *Topics in Communication Theory,* Mc Graw Hill, New York, 1965, pp 22-23.

[6] Whalen, A.D. *Detection of Signals in Noise,* Academic Press, 1971, pp 125-154.

[7] Mascarenhas, N.D.A. and Prado, L.O.C., Edge Detection in Images: A Statistical Formulation, Internal Report # 1058-NTE/094, Instituto de Pesquisas Espaciais, São José dos Campos, Brazil, July 1977 (in Portuguese).

[9] Hildebrand, F.B. *Introduction to Numerical Analysis,* Mc Graw Hill, New York, 1956, pp 324-330.

[10] Abramovitz, M. and Stegun, I. *Handbook of Mathematical Functions,* Dover, New York, 1965.

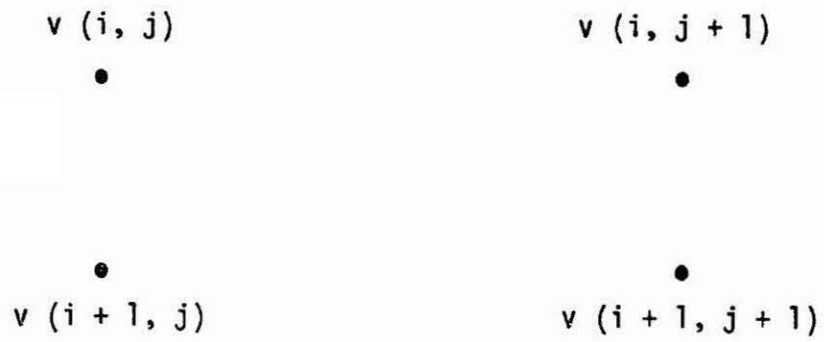

Fig. 1 - Set of Pixels for Edge Detection

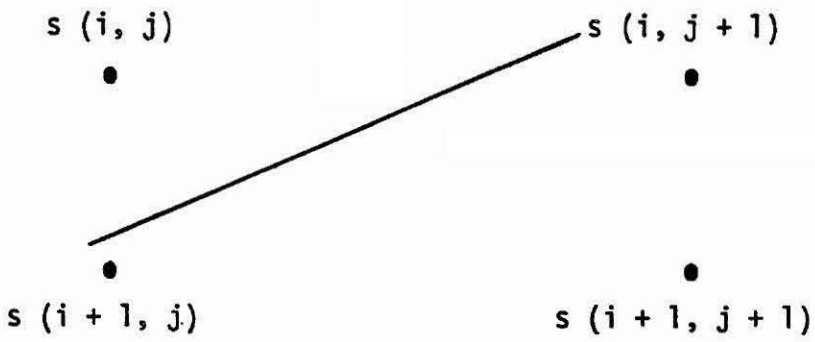

Fig. 2 - Edge of the 1st Type (diagonal)

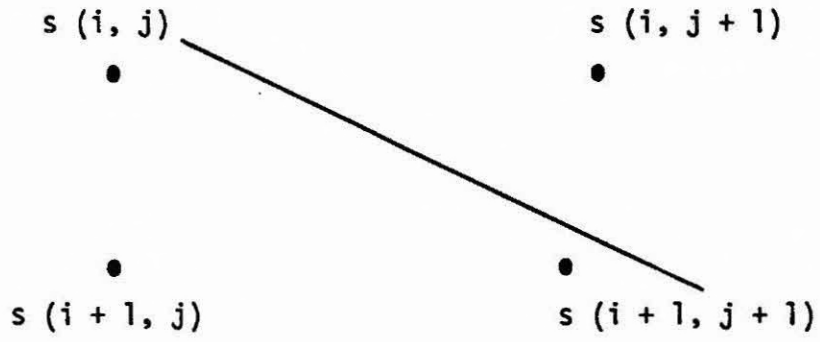

Fig. 3 - Edge of the 2nd Type (diagonal)

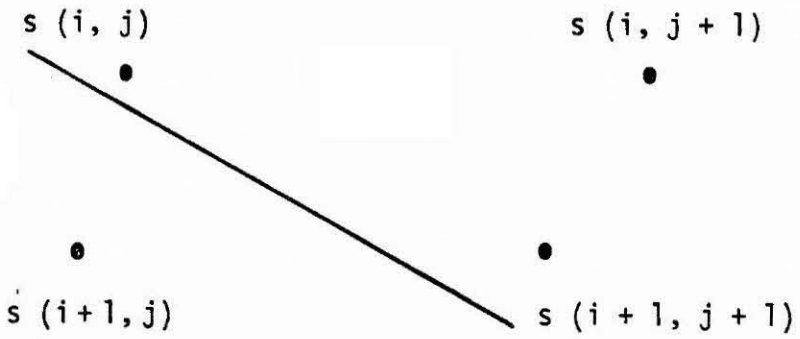

Fig. 4 - Edge of the 3rd Type (diagonal)

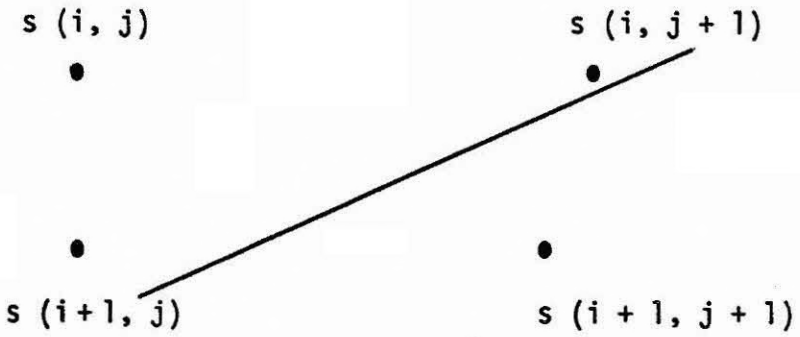

Fig. 5 - Edge of the 4th Type (diagonal)

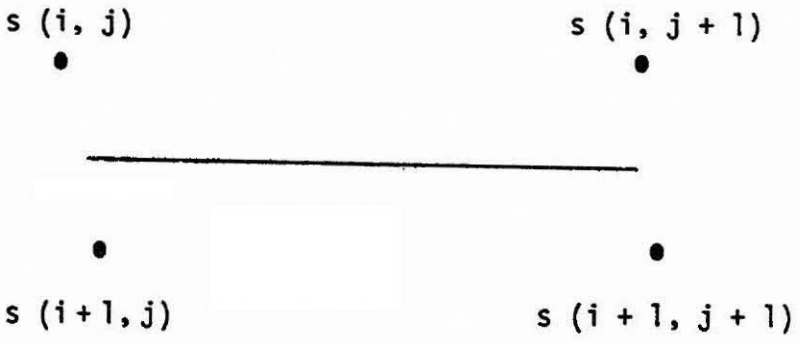

Fig. 6 - Edge of the 5th Type (horizontal)

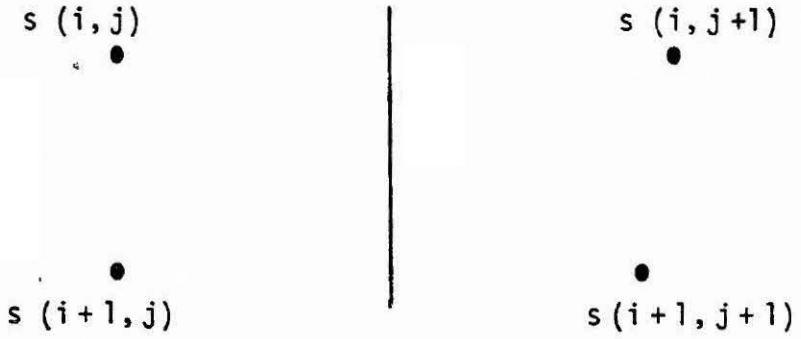

Fig. 7 - Edge of the 6th Type (vertical)

Fig. 8 - Example of Overlapping of Hypotheses

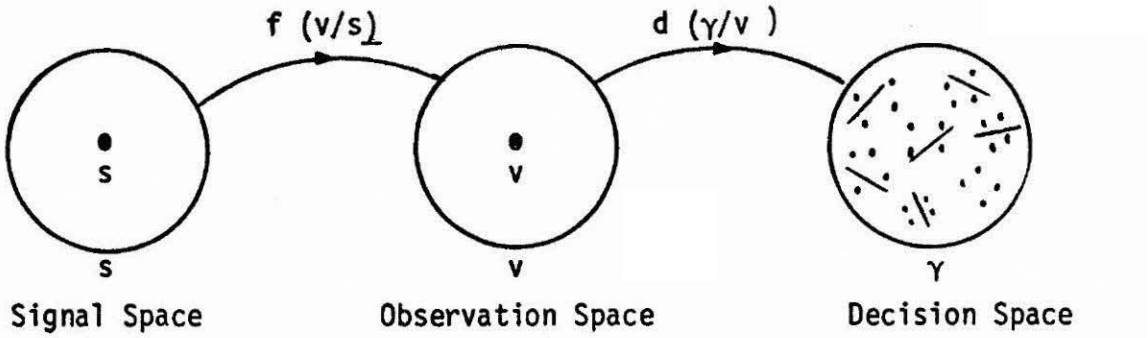

Fig. 9 - Spaces for the Detection Problem

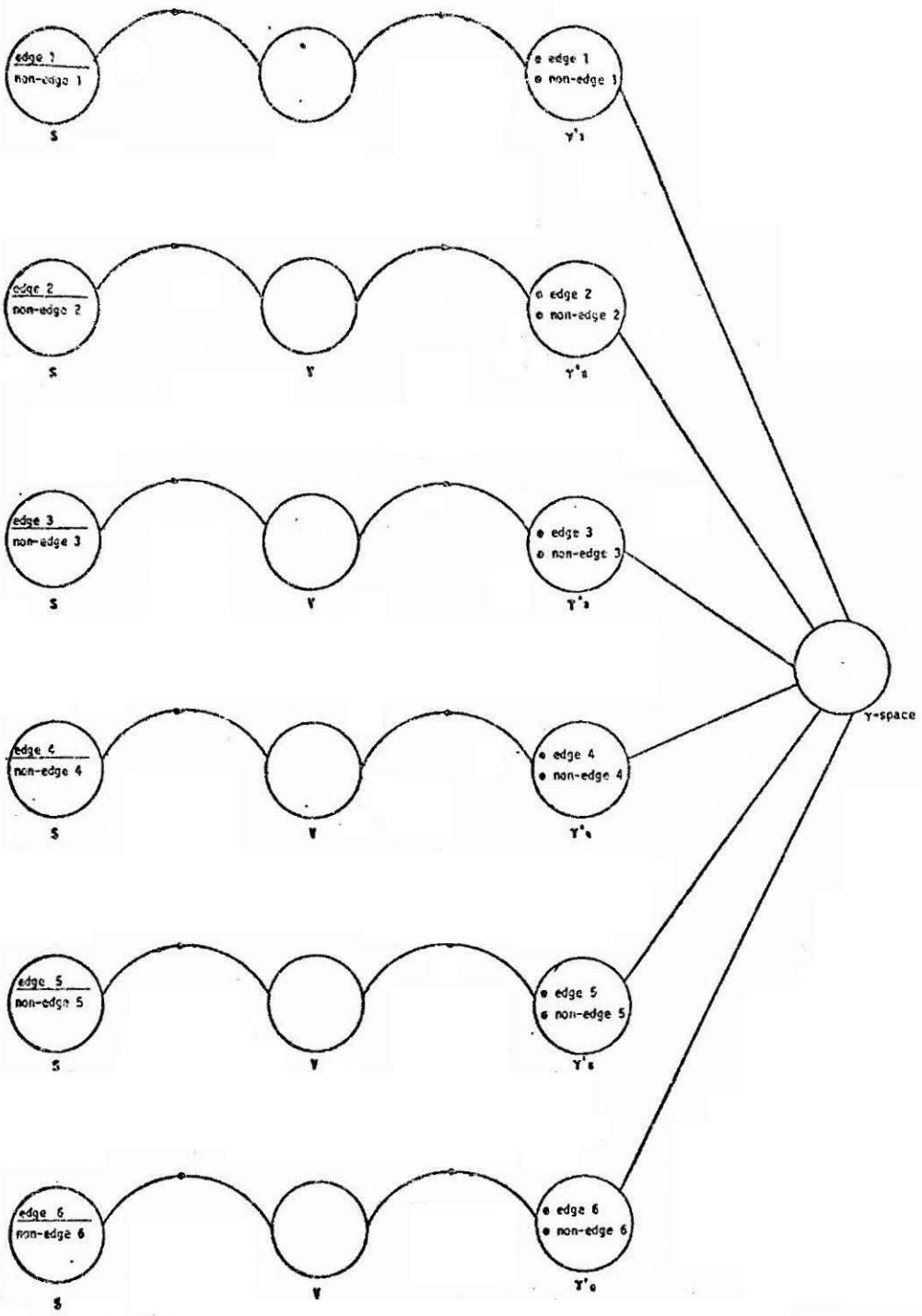

Fig. 10 - Diagram of the Model for Suboptimal Scheme

Fig. 11
Original
Cartoon
Image

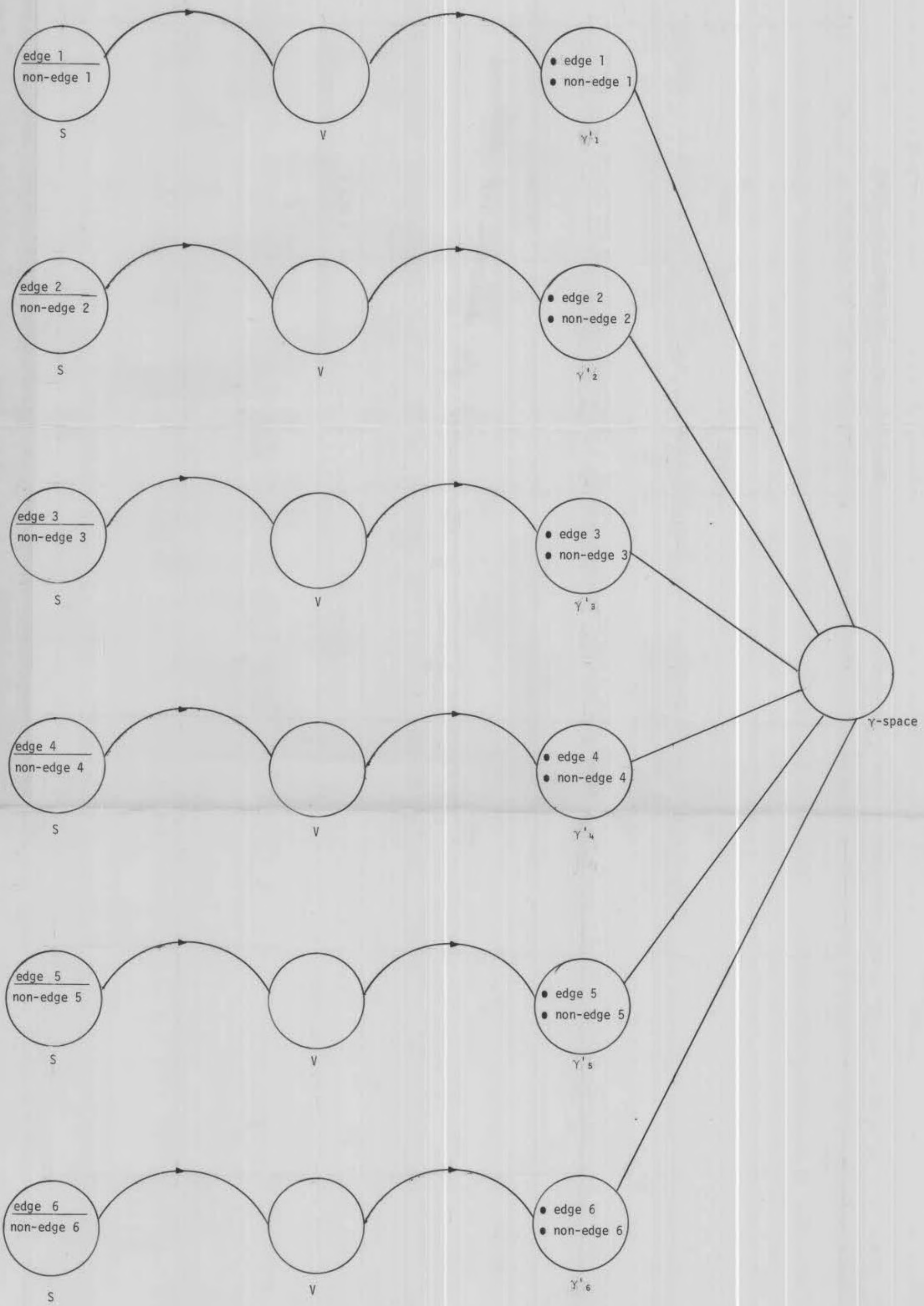
edge 1
non-edge 1
S
V
• edge 1
• non-edge 1
γ'1
edge 2
non-edge 2
S
V
• edge 2
• non-edge 2
γ'2
edge 3
non-edge 3
S
V
• edge 3
• non-edge 3
γ'3
edge 4
non-edge 4
S
V
• edge 4
• non-edge 4
γ'4
γ-space
edge 5
non-edge 5
S
V
• edge 5
• non-edge 5
γ'5
edge 6
non-edge 6
S
V
• edge 6
• non-edge 6
γ'6

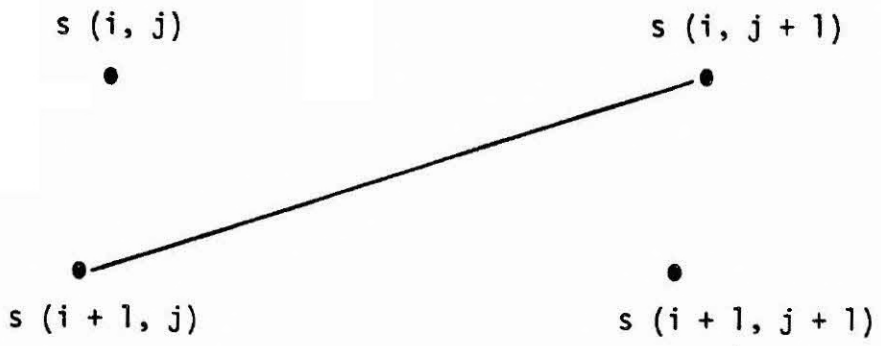

Fig. 12 - Edge of the 1st Type (diagonal)

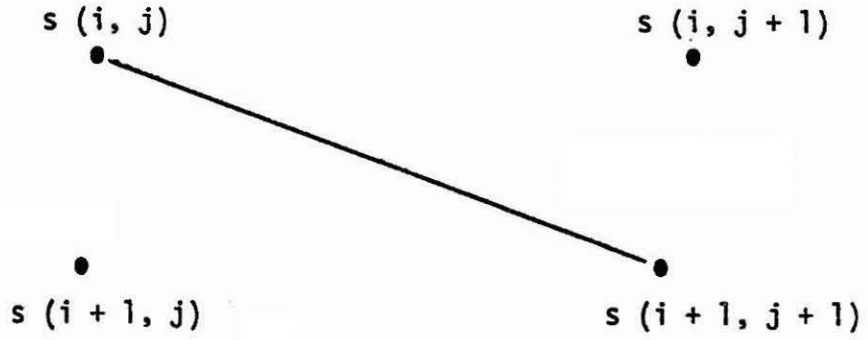

Fig. 13 - Edge of the 2nd Type (diagonal)

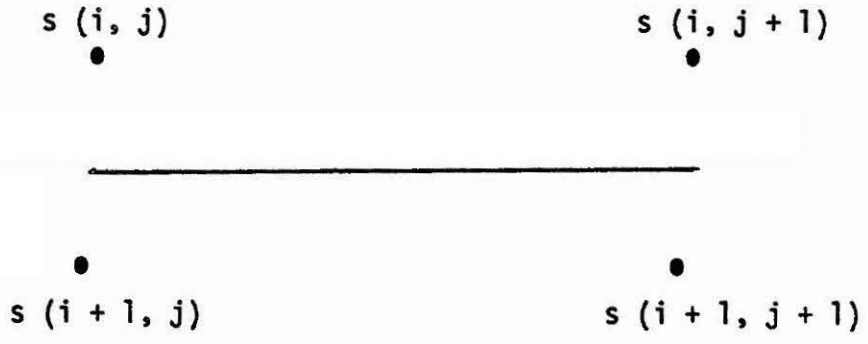

Fig. 14 - Edge of the 3rd Type (horizontal)

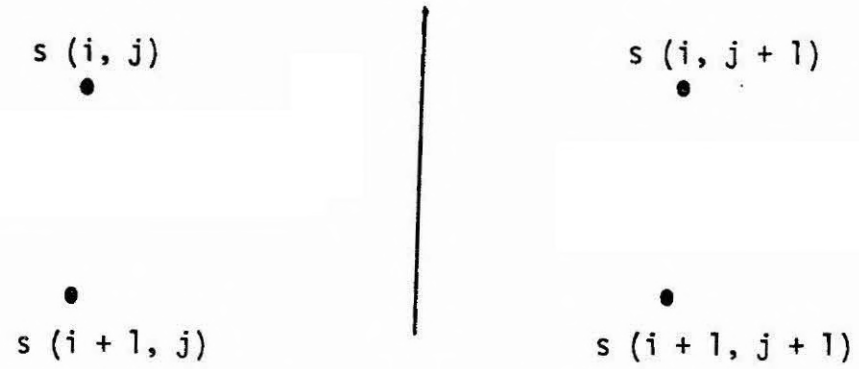

Fig. 15 - Edge of the 4th Type (vertical)

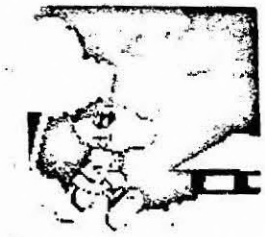

Fig. 16
Cartoon
Image
SNR = 100

Fig. 17
Edges in
Cartoon
Image
SNR = 100

Fig. 18
Cartoon
Image
SNR = 30

Fig. 19
Edges in
Cartoon
Image
SNR = 30

Fig. 20
Cartoon
Image
SNR = 10

Fig. 21
Edges in
Cartoon
Image
SNR = 10

Fig. 22
Cartoon
Image
SNR = 5

Fig. 23
Edges in
Cartoon
Image
SNR = 5
C_{10} = 1

Fig. 24
Edges in
Cartoon
Image
SNR = 5
C_{10} = 1,5

Fig. 25
Gradient
(SNR = 10)

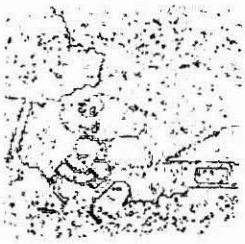

Fig. 26
Gradient
(SNR = 5)

Fig. 27
Satellite
Picture

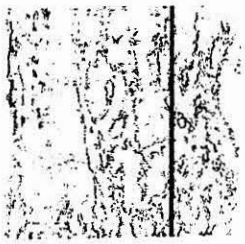

Fig. 28
Edges in
Satellite
Picture
(32 Levels)

Fig. 29
Edges in
Satellite
Picture
(8 Levels)